available at www.sciencedirect.com
journal homepage: www.europeanurology.com

European Association of Urology

Surgery in Motion

Multiparametric Magnetic Resonance Imaging for the Detection of Clinically Significant Prostate Cancer: What Urologists Need to Know. Part 2: Interpretation

Bas Israël[a], *Marloes van der Leest*[a], *Michiel Sedelaar*[b], *Anwar R. Padhani*[c], *Patrik Zámecnik*[a], *Jelle O. Barentsz*[a,*]

[a] *Department of Radiology and Nuclear Medicine, Radboud university medical center, Radboud Institute for Health Sciences, Nijmegen, The Netherlands;* [b] *Department of Urology, Radboud university medical center, Radboud Institute for Health Sciences, Nijmegen, The Netherlands;* [c] *Paul Strickland Scanner Centre, Northwood, UK*

Article info

Article history:
Accepted October 21, 2019

Associate Editor: Alexandre Mottrie

Keywords:
Prostate cancer
Magnetic resonance imaging
Multiparametric magnetic resonance imaging
Interpretation prostate imaging reporting and data system version 2
Prostate imaging reporting and data system

Please visit www.europeanurology.com and www.urosource.com to view the accompanying video.

Abstract

Background: There is large variability among radiologists in their detection of clinically significant (cs) prostate cancer (PCa) on multiparametric magnetic resonance imaging (mpMRI).
Objective: To reduce the interpretation variability and achieve optimal accuracy in assessing prostate mpMRI.
Design, setting, and participants: How the interpretation of mpMRI can be optimized is demonstrated here. Whereas part 1 of the "surgery-in-motion" paper focused on acquisition, this paper shows the correlation between (ab)normal prostate anatomical structures and image characteristics on mpMRI, and how standardized interpretation according to Prostate Imaging Reporting and Data System version 2 (PI-RADS v2) should be performed. This will be shown in individual patients.
Surgical procedure: To detect csPCa, three mpMRI "components" are used: "anatomic" T2-weighted imaging, "cellular-density" diffusion-weighted imaging, and "vascularity" dynamic contrast-enhanced MRI.
Measurements: Based on PI-RADS v2, the accompanying video shows how mpMRI interpretation is performed. Finally, the role of mpMRI in detecting csPCa is briefly discussed and the main features of the recently introduced PI-RADS v2.1 are evaluated.
Results and limitations: With PI-RADS v2, it is possible to quantify normal and abnormal anatomical structures within the prostate based on its imaging features of the three mpMRI "components." With this knowledge, a more objective evaluation of the presence of a csPCa can be performed. However, there still remains quite some space to reduce interobserver variability.
Conclusions: For understanding the interpretation of mpMRI according to PI-RADS v2, knowledge of the correlation between imaging and (ab)normal anatomical structures on the three mpMRI components is needed.
Patient summary: This second surgery-in-motion contribution shows what structures can be recognized on prostate magnetic resonance imaging (MRI). How a radiologist performs his reading according to the so-called Prostate Imaging Reporting and Data System criteria is shown here. The main features of these criteria are summarized, and the role of prostate MRI in detecting clinically significant prostate cancer is discussed briefly.

* Corresponding author. Department of Radiology and Nuclear Medicine, Radboud University Nijmegen Medical Center, P.O. Box 9101, Nijmegen, The Netherlands. Tel. +31243619196, +31625015262, Fax: +31243540866.
E-mail address: jelle.barentsz@radboudumc.nl (J.O. Barentsz).

https://doi.org/10.1016/j.eururo.2019.10.024

1. Prostate multiparametric magnetic resonance imaging

Magnetic resonance imaging (MRI) is a noninvasive imaging technique that uses the interaction between radiofrequency pulses, a strong magnetic field, and body tissue, to obtain images of planes inside the body. Compared with other imaging modalities, such as ultrasound and computed tomography (CT) scanning, MRI is superior in soft tissue imaging [1]. Unlike x-rays and CT scans, MRI uses no radiation. The recommended technique of MRI in prostate cancer (PCa) is multiparametric-MRI (mpMRI), which includes high-resolution T2-weighted (T2W) images to depict prostate anatomy and two functional MRI techniques, including diffusion-weighted imaging (DWI) to display cell density and dynamic contrast-enhanced MRI (DCE-MRI) that shows vascularity.

Clinical indications for mpMRI of the prostate include detection and localization of primary PCa for guidance of MRI-directed biopsy (MRDB), local staging, assessment of suspected PCa recurrence, active surveillance, and local treatment (eg, surgery, radiation therapy, and focal therapy) [2–7].

1.1. T2-weighted imaging

T2W imaging (T2WI) shows anatomic-morphologic features of the prostate and morphologic-pathologic structures. T2W images are acquired preferably in three perpendicular planes (axial, coronal, and sagittal). These show the anatomic prostate zonal anatomy and the relation of the prostate to its surrounding structures. T2WI is ideal to differentiate between the high-signal peripheral zone (PZ), the heterogeneous mixed-signal transition zone (TZ), and the low-signal central zone (CZ). The high-signal of the PZ is caused by cystic degeneration with high fluid content and is usually surrounded by a thin hypointense rim that represents the pseudocapsule. This rim is an important landmark for tumor staging [8]. The TZ usually has a heterogeneous mixed signal due to the various stages of the benign prostatic hypertrophy (BPH) nodules (Fig. 1). BPH can be degenerative or can show cellular hypertrophy. On T2WI, this BPH-changed TZ is often referred to as "organized chaos." The CZ has more dense fibrous tissue and, therefore, a low signal on T2WI.

On T2WI, lesions can be anatomically localized, and their shape, form, and size are assessed. Zonal distinction of the prostate is important as approximately 70–75% of PCa cases arise from the PZ, and the Prostate Imaging Reporting and Data System (PI-RADS) assessment is zonal based [9–11]. The high-signal PZ may be disrupted as an area of a lower signal due to the presence of PCa. However, PCa can also present as isosignal areas or nonfocal mildly hypointense abnormalities. Low-grade PCa or nonmalignant conditions, such as scar tissue, hemorrhage, atrophy, postradiation changes, and (granulomatous) prostatitis, frequently have a low signal intensity; thus, based on its signal on T2WI, it cannot be differentiated from clinically significant (cs) PCa [12,13]. To some extent, using anatomic-morphologic structures for the differentiation of csPCa from low-grade PCa and benign pathology is possible [7]. A focal, round, or irregular structure is more likely to be csPCa,

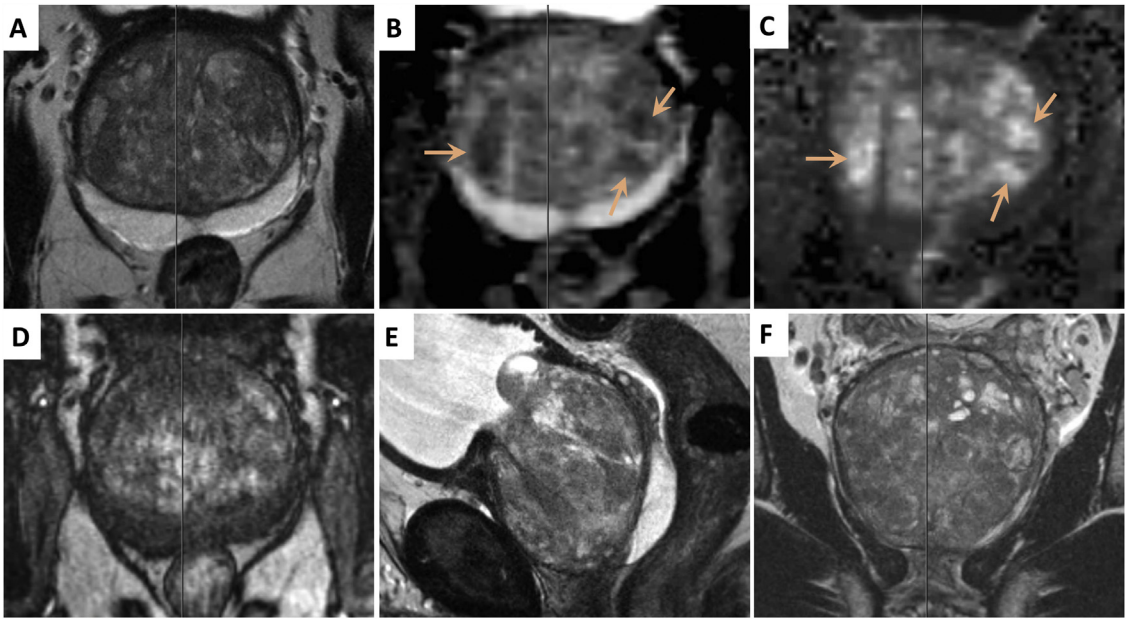

Fig. 1 – PI-RADS 1 (BPH) assessment of a patient aged 56 yr, having cT0, PSA 13, 219 cc, PSAd 0.06. (A) Axial, (E) sagittal, and (F) coronal T2W images show well-circumscribed nodules in the TZ, which are surrounded by a low-signal rim. Normal (bright) PZ. Some nodules show restricted diffusion: "dark" on (B) axial ADC map and" white" on (C) *b* 1400 (arrows). For BPH, this is normal. (D) Axial DCE images show minimal "pop-corn" enhancement that is typical for BPH nodules. This is scored as "–". Thus the score T2W/DWI/DCE is 1/1/–, with PI-RADS v2.1 category 1 (BPH). TRUS biopsy revealed no abnormalities. ADC = apparent diffusion coefficient; BPH = benign prostatic hypertrophy; DCE = dynamic contrast enhanced; DWI = diffusion-weighted imaging; PI-RADS = Prostate Imaging Reporting and Data System; PSA = prostate-specific antigen; PSAd = PSA density; PZ = peripheral zone; TRUS = transrectal ultrasound; T2W = T2 weighted; TZ = transition zone.

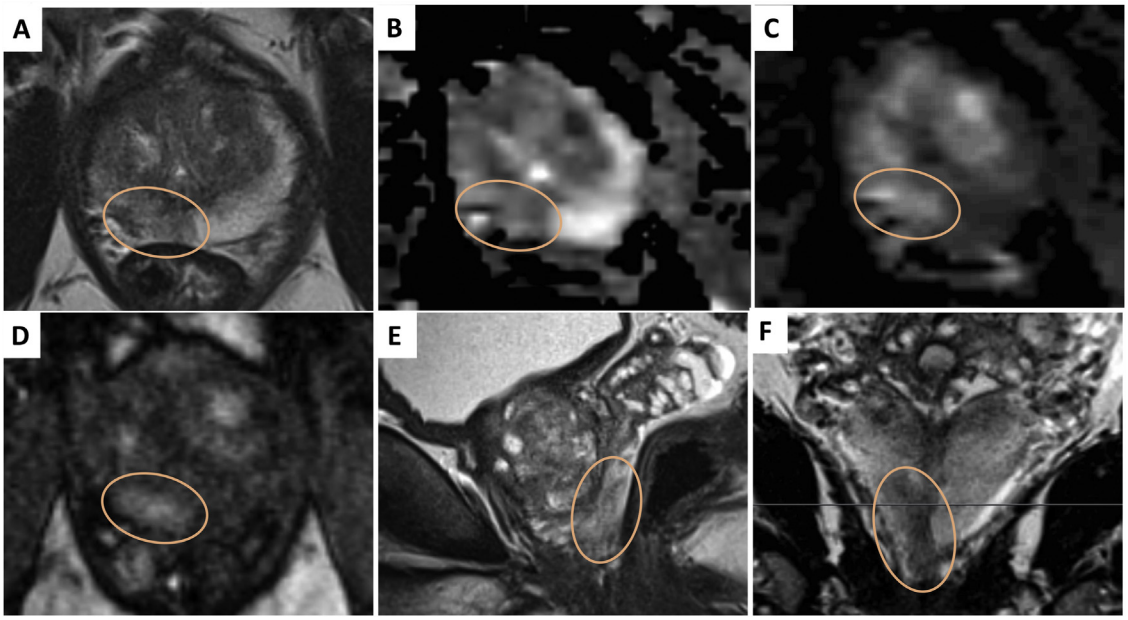

Fig. 2 – PI-RADS 2 (prostatitis) assessment of a patient aged 61 yr, having cT0, PSA 5.1, 63 cc, PSAd 0.08. (A) Axial, (E) sagittal, and (F) coronal T2W images show linear and wedge-shaped mild hypointensities of the right PZ (orange circle). (B) Indistinct diffuse minimal hypointense signal on ADC map and (C) no "high signal" on *b* 1400 (orange circles). (D) DCE images show early enhancement (bright signal) of the right PZ (orange circle). Score: T2W/DWI/DCE: 2/2/+. This results in PI-RADS v2.1 category 2 (prostatitis). TRUS biopsy showed chronic inflammation. ADC = apparent diffusion coefficient; DCE = dynamic contrast enhanced; DWI = diffusion-weighted imaging; PI-RADS = Prostate Imaging Reporting and Data System; PSA = prostate-specific antigen; PSAd = PSA density; PZ = peripheral zone; TRUS = transrectal ultrasound; T2W = T2 weighted; TZ = transition zone.

whereas prostatitis is marked by a wedge-shaped and more diffuse appearance (Fig. 2) [14,15]. The diagnosis of csPCa in the TZ imposes a greater challenge than in the PZ. Features indicative of TZ cancers are ill-defined margins; focal homogeneous T2 intermediate-low signal ("erased charcoal drawing sign"); noncircumscribed, lenticular, or fusiform shape; and invasion of the surrounding structures ("disruption of organized chaos"; Fig. 3) [7]. To determine whether an abnormal region is suspicious for csPCa, T2WI should be used in conjunction with the other two functional imaging techniques.

1.2. *Diffusion-weighted imaging*

On T2WI, differentiation of csPCa from low-grade PCa, fibrous tissue, inflammation, postbiopsy hematoma, and glandular BPH nodules is difficult. Thus, DWI is needed for further evaluation of tissue characteristics. DWI is the most important functional imaging technique because it corresponds to histopathologic findings [16–19]. DWI shows the velocity (diffusion) of intracellular water. In dense cellular tissue, this velocity is reduced; therefore, diffusion is restricted. This is visible as a low signal (black) on the DWI-derived velocity map: the apparent diffusion coefficient (ADC) map [20,21]. Low cell density has a high signal (white) on the ADC map. Another DWI-derived image that is used is the high *b*-value ($\geq$1400 s/mm^2) image. On these images, high cell density has a high signal (white) and low cell density is dark [22,23]. On DWI, the normal PZ has a high signal (white) due to its high content of fluid-filled glandular structures and high velocity of water molecules [24,25]. Clinically significant PCa replaces healthy glandular tissue and has high cell density; therefore, it is visible as a low signal on the ADC map (restricted diffusion). There is an inverse relationship between ADC value and Gleason score (GS), that is, decreasing ADC values (low signal) correlate significantly with increasing GSs [26–28]. However, in the TZ, BPH can also show restricted diffusion; hence, DWI is more accurate for csPCa detection in the PZ than in the TZ [29]. A focal lesion is more likely to be csPCa than a more diffuse lesion (eg, prostatitis). Finally, DWI is highly susceptible to artifacts. Bowel peristalsis, total hip prosthesis, or gas in the rectum (susceptibility artifacts) can limit DWI quality.

1.3. *DCE and T1-weighted imaging*

DCE-MR images are T1-weighted (T1W) images that show tissue enhancement (vascularization) after bolus injection of an MR contrast agent. Owing to tumor angiogenesis and higher vessel permeability, both low-grade PCa and csPCa, cellular-BPH, and inflammation show earlier and more pronounced enhancement compared with other prostate tissue [30,31]. Thus, accurate differentiation of benign prostate structures such as (highly vascularized) prostatitis in the PZ or (highly perfused) cellular BPH in the TZ from csPCa is limited. DCE-MRI is of essential value for the detection of local recurrences (eg, postradiotherapy or after radical prostatectomy) [4,32]. In untreated patients, DCE-MRI helps identify prostatitis and is of value in "equivocal"

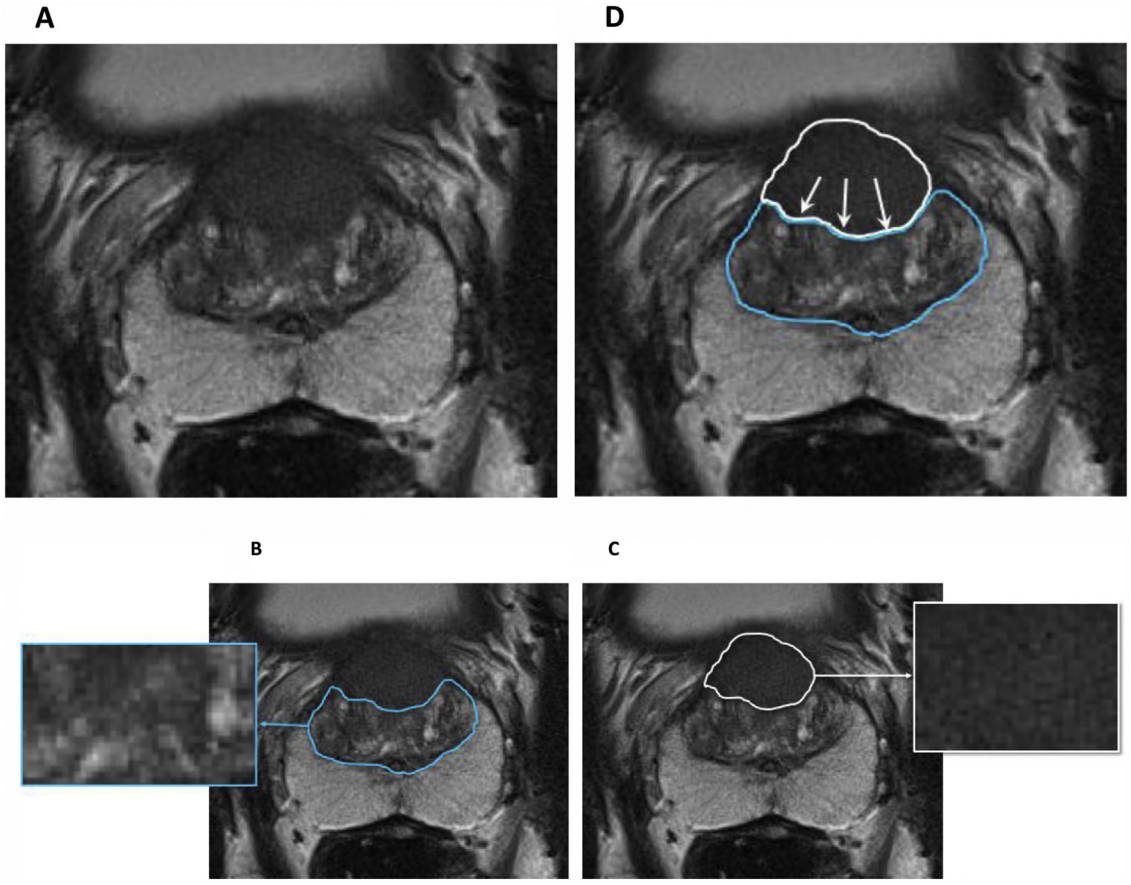

Fig. 3 – PI-RADS 5 TZ lesion: disruption of BPH ("organized chaos") by ISUP grade 3 PCa ("erased charcoal"). (A) Axial T2W image through midprostate shows a normal bright PZ. (B) BPH in the TZ is visible as "organized chaos" (blue area, magnified in box). (C) Ventral to the BPH a homogeneous intermediate signal "erased charcoal" area is visible (white, magnified in box). (D). This area (TZ PI-RADS 5 lesion; ISUP grade 3 on targeted biopsy) shows "disruption of organized chaos" (arrows). BPH = benign prostatic hypertrophy; ISUP = International Society of Urological Pathology PCa = prostate cancer; PI-RADS = Prostate Imaging Reporting and Data System; PZ = peripheral zone; T2W = T2 weighted; TZ = transition zone.

findings in the PZ. Unenhanced (precontrast) T1W imaging is the only technique to identify postbiopsy hemorrhage by its high T1W signal [33].

2. MRI interpretation

2.1. *PI-RADS version 2*

In 2012, the prostate MR working group of the European Society of Urogenital Radiology (ESUR) initiated a guideline (PI-RADS v1) to standardize mpMRI acquisition, and interpretation and reporting of mpMRI scans [14]. A second version of PI-RADS (v2) was developed by a joint steering committee of the ESUR, the American College of Radiology, and the AdMeTech Foundation [7]. More recently, an updated version (v2.1) was published [34]. This updated version aimed to further simplify the assessment and reporting, as well as to reduce interpretation variability of prostate mpMRI.

PI-RADS is a risk assessment tool based on a standardized evaluation method to predict the likelihood that csPCa is present. Each detected lesion is scored separately using a standardized description for the three individual MRI techniques: T2WI, DWI, and DCE-MRI. Thereafter, they are combined to give an overall assessment category score, from 1 (csPCa is highly unlikely to be present) to 5 (csPCa is highly likely to be present; Table 1). PI-RADS v2.1

Table 1 – PI-RADS v2 assessment categories and risk of (cs)PCa.

PI-RADS v2 categories	Risk of csPCa	% PCa [36,40,42,43,46,48,59,60]	% csPCa (ISUP grade ≥2)
1–2	(Very) low	13–24	3–12
3	Equivocal	34–50	4–27
4	High	60–77	32–60
5	Very high	91–97	67–83

csPCa = clinically significant prostate cancer; ISUP = International Society of Urological Pathologt PCa = prostate cancer; PI-RADS v2 = Prostate Imaging Reporting and Data System version 2.

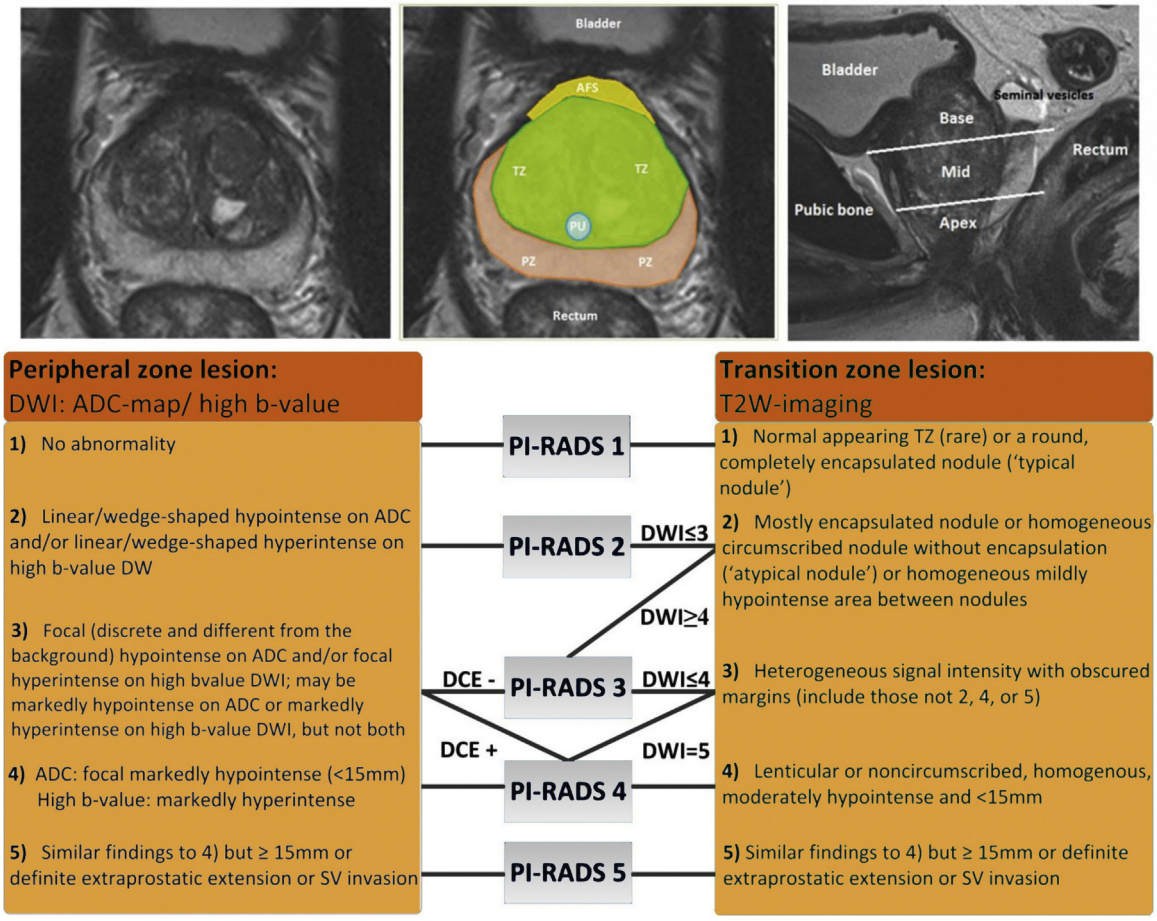

Fig. 4 – Prostate zonal anatomy and PI-RADS v2.1 assessment. ADC = apparent diffusion coefficient; AFS = anterior fibromuscular stroma; DCE = dynamic contrast enhanced; DWI = diffusion-weighted imaging; PI-RADS = Prostate Imaging Reporting and Data System; SV = seminal vesicle; PU = prostatic urethra; PZ = peripheral zone; T2W = T2 weighted; TZ = transition zone.

emphasizes the dominant role of DWI as the parameter for any suspicious lesion(s) found in the PZ and T2WI, in combination with DWI in TZ lesions (Fig. 4). DCE-MRI scores are a binary assessment, and its role is limited to upgrading DCE-MRI–positive lesion(s) in the PZ from PI-RADS category 3 to 4. A more precise division of prostate sectors was proposed [15,34].

2.2. How to score lesions (video)

For optimal reading, a dedicated workstation should be used that shows all images in one view: triplanar T2WI, axial ADC map, axial high *b*-value DWI, and axial (cine-loop) DCE-MRI. In addition, a cross-correlation tool, such as a "cross-hair" should be used, which enables a specific area in one view to be evaluated on all images.

First, image quality must be assessed. If the quality is insufficient, either this should be reported (as PI-RADS category X) or the patient must undergo additional imaging to obtain better images. Feedback should be given to the technologist and corrective measures should be implemented. Then the maximal prostate dimensions on T2WI are measured in three perpendicular planes (anterior-posterior [AP], left-right [LR], and cranial-caudal [CC]), and prostate volume ($AP \times LR \times CC \times 0.52$) and prostate-specific antigen (PSA) density (PSAd = PSA divided by prostate volume) are calculated. After appropriate adjustments of the contrast and brightness (so-called "window" and "center") of the images, suspicious lesions are looked for on all T2WI planes.

Before any lesion is scored (characterized), it needs to be detected. PI-RADS is agnostic about lesion detection method. We suggest that T2WI, high *b*-value DWI, and early post–contrast enhancement images be evaluated initially for any lesion(s) that could represent csPCa, based on morphologic findings, signal characteristics, or enhancement patterns. These features need not be confined to those described for scoring purposes; lesions or regions that could be abnormal need to be detected prior to PI-RADS v2.1 characterization. However, special attention should be placed on TZ lesions that show "erased charcoal" or "disruption of organized chaos," and PZ lesions that are "black" on the ADC-map and "white" on the high *b*-value DWI. These should be evaluated for a likelihood of csPCa using PI-RADS.

Location assessment of a lesion in either the PZ or the TZ/CZ is of utmost importance, as these zones have a different

"dominant" sequence according to PI-RADS. If a lesion is identified on T2WI, its signal intensity, size, and appearance should be determined on the ADC map and the high *b*-value ($b \geq 1400 s/mm^2$) DWI.

A focal mass in the PZ with a low signal on the ADC map and a high signal on the high *b*-value DWI has a PI-RADS 4 or 5 assessment, with the distinction being determined by size (cutoff: 15 mm) or extracapsular extension (Fig. 5–7). If a TZ has an "erased charcoal" appearance and/or there is "disruption of organized chaos" on T2WI, or if an anterior TZ lesion has a "lenticular shape," then the PI-RADS assessment is also 4 or 5 (Fig. 6). Usually, a csPCa located in the TZ also has a low signal on the ADC map and a high signal on high *b*-value DWI. However, cellular BPH may have

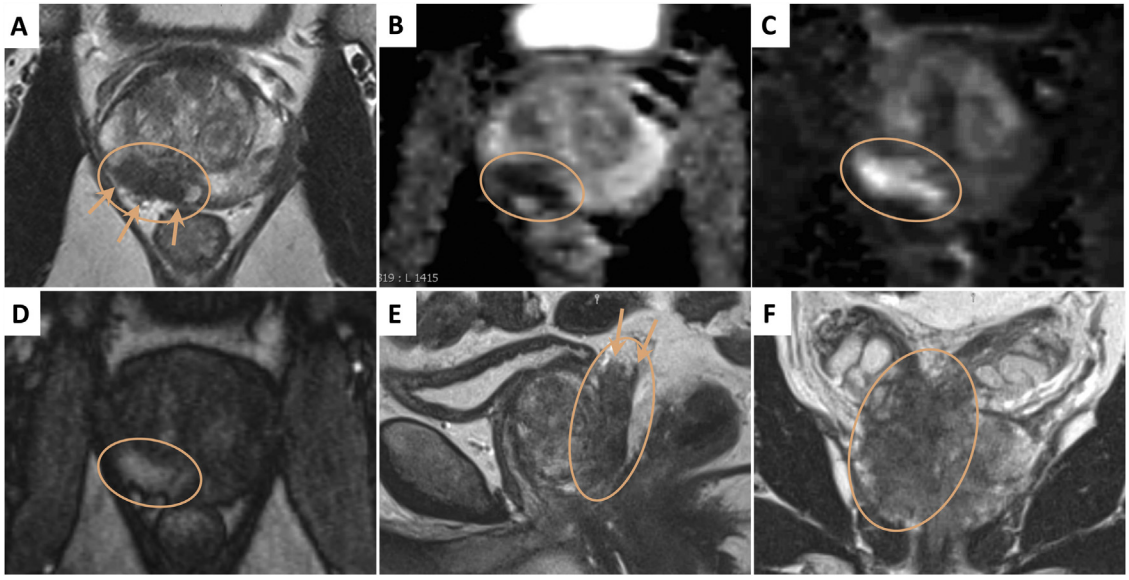

Fig. 5 – PI-RADS 5 assessment of a patient aged 74 yr, with cT2 on the right side, PSA 7.1, 64 cc, PSAd 0.11). (A) Axial, (E) sagittal, and (F) coronal T2W images show low-signal lesion midprostate, PZ, 6–9 o'clock (orange circles). ADC shows a (B) focal "black" area with a low ADC value (600) and (C) focal "white" area on *b* 1400. (D) On DCE image, this lesion shows early focal enhancement. (A) axial T2W image shows extracapsular extension (arrows) MRI stage T3a. (E) Sagittal T2W image shows seminal vesicle infiltration (arrows) MRI stage T3b. Transperineal fusion biopsy showed PCa ISUP grade 3. Score: T2W/DWI/DCE: 5/5/+. This results in PI-RADS v2.1 category 5 (high risk for csPCa). ADC = apparent diffusion coefficient; csPCa = clinically significant prostate cancer; DCE = dynamic contrast enhanced; DWI = diffusion-weighted imaging; ISUP = International Society of Urological Pathology; MRI = magnetic resonance imaging; PCa = prostate cancer; PI-RADS = Prostate Imaging Reporting and Data System; PSA = prostate-specific antigen; PSAd = PSA density; PZ = peripheral zone; T2W = T2 weighted.

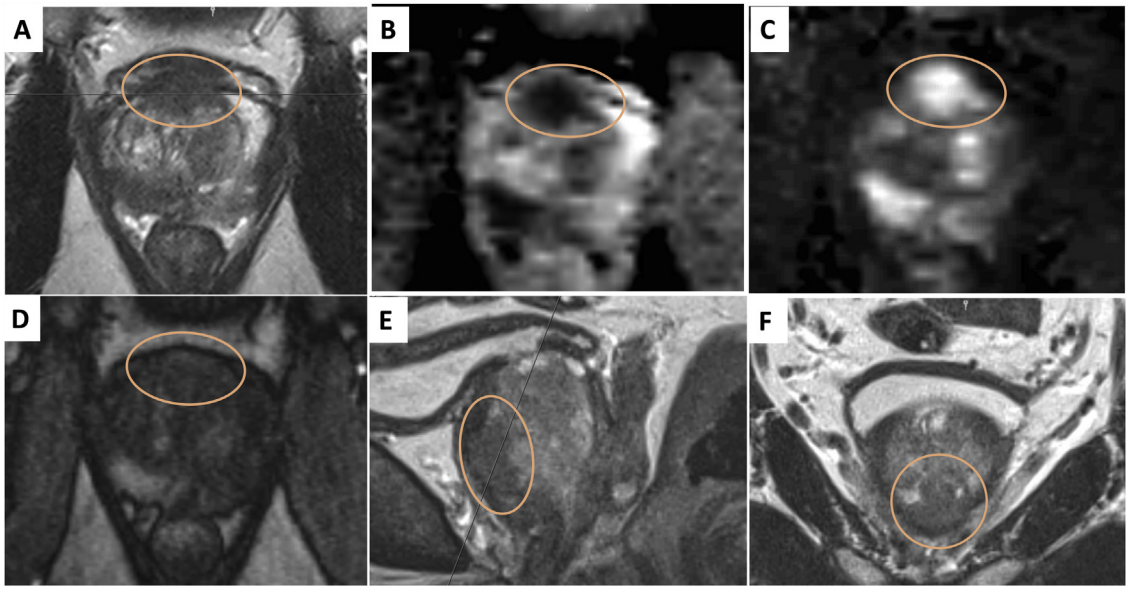

Fig. 6 – Same patient as in Fig. 5, lesion #2: PI-RADS 5. (A) Axial, (E) sagittal, and (F) coronal T2W images show a low-signal lesion apex to midprostate, TZ, 11–1 o'clock (orange circles), with diameter >15 mm. (B) ADC shows a focal "black" area with a low ADC, which is (C) a focal "white" area on *b* 1400. (D) DCE image does not show early focal enhancement. Score: T2W/DWI/DCE: 5/5/–. This results in PI-RADS v2.1 category 5. Transperineal fusion biopsy showed PCa ISUP grade 2. ADC = apparent diffusion coefficient; DCE = dynamic contrast enhanced; DWI = diffusion-weighted imaging; ISUP = International Society of Urological Pathology; PCa = prostate cancer; PI-RADS = Prostate Imaging Reporting and Data System; T2W = T2 weighted; TZ = transition zone.

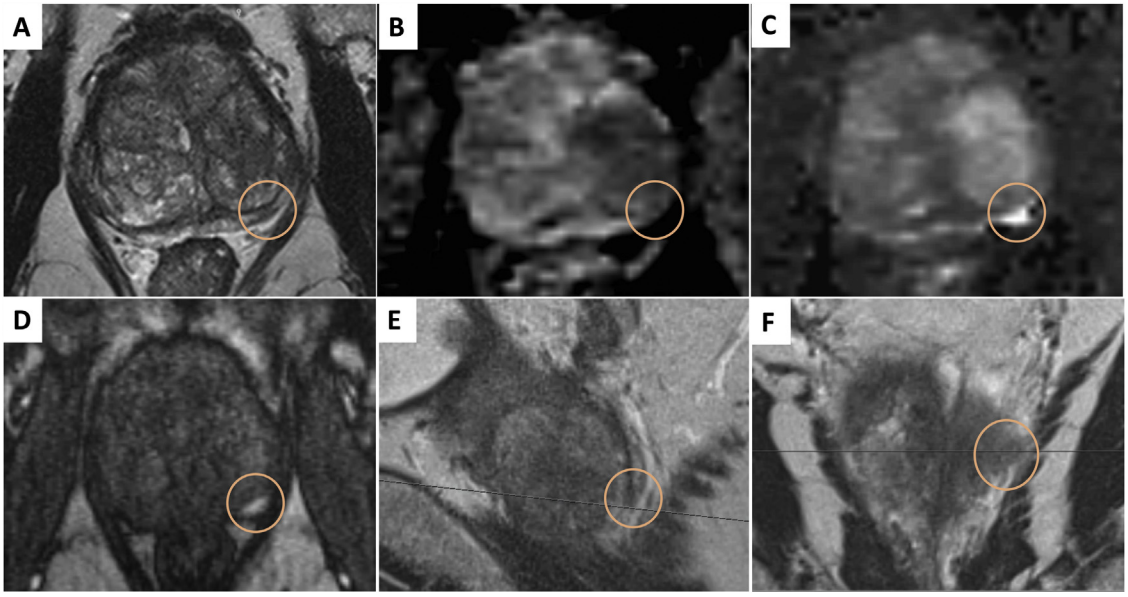

Fig. 7 – PI-RADS 4 assessment of a patient aged 70 yr, with cT0, PSA 9.8, 115 cc, PSAd 0.08. (A) Axial, (E) sagittal, and (F) coronal T2W images show a $3 \times 5 \times 8$ mm^3 small focal low-signal-intensity lesion at midprostate, PZ, 4–5 o'clock (lesion is within orange circles). DWI shows (B) no focal low signal on ADC map and (C) a focal high signal intensity on *b* 1400. (D) The DCE-MRI shows marked early focal enhancement. Score: T2W/DWI/DCE: 4/3/+. This results in PI-RADS v2.1 category 4 (at risk for csPCa). MR-TRUS fusion biopsy showed PCa ISUP grade 4. ADC = apparent diffusion coefficient; csPCa = clinically significant prostate cancer; DCE = dynamic contrast enhanced; DWI = diffusion-weighted imaging; ISUP = International Society of Urological Pathology; MRI = magnetic resonance imaging; PCa = prostate cancer; PI-RADS = Prostate Imaging Reporting and Data System; PSA = prostate-specific antigen; PSAd = PSA density; PZ = peripheral zone; TRUS = transrectal ultrasound; T2W = T2 weighted.

similar appearance on DWI, and the corresponding T2WI should therefore be determinant. In the TZ, partially encapsulated or circumscribed, encapsulated nodules (T2WI score of 2) with clearly restricted diffusion (DWI score 4 or 5) receive a final score of PI-RADS 3. TZ lesions with a T2WI score of 3 and a DWI score of 5 (ie, >1.5 cm) are assessed as PI-RADS 4 lesions (Fig. 4).

Finally, the DCE-MRI sequence must be evaluated to see whether early enhancement in the PZ matches with a wedge-shaped or diffuse intermediate signal ADC lesion (ie, prostatitis), or a detected/undetected focal lesion. If a lesion in the PZ is scored 3 on DWI but shows early focal enhancement, the final PI-RADS assessment is 4 (Fig. 7).

Up to four lesions are assessed. The lesion with the highest PI-RADS score is called the "index lesion." Its location, size, lowest ADC value, and risk of extraprostatic extension (either extracapsular extension or seminal vesicle infiltration) are reported.

2.3. Clinical parameters

Although the PI-RADS v2.1 score is assigned solely on the mpMRI assessments, clinical (risk) factors should also be considered, as these are of importance for decision making. The following clinical information should be available to radiologists at the time of reporting: digital rectal examination findings, family history, PSA history and most recent PSA level, previous biopsy status (in case of a prior biopsy, date and histopathologic findings), prior prostate and/or pelvic surgery, and medication affecting the PSA level.

The MRI-derived PSAd is important to know during the interpretation of the images. If the PSAd is above a certain cutoff level (eg, ≥0.15 ng/ml/ml), the radiologist should be very cautious not to miss a csPCa and should seek an explanation for the elevated PSAd, for example, prostatitis or csPCa [35]. It is important to remember that diagnostic decisions regarding the need for a biopsy should take into account all clinical variables and the overall PI-RADS imaging assessment.

2.4. Nonsuspicious mpMRI (PI-RADS categories 1 and 2)

Circumscribed low-signal or mixed-signal (encapsulated) nodules on T2WI represent normal BPH (PI-RADS 1; Fig. 1). Protruding or exophytic BPH nodules can occasionally be found in the PZ, often without continuity with BPH within the TZ [12,36–38]. In these cases, interpretation can be difficult. Assessment of the other T2WI planes (coronal and sagittal) can aid in verifying its nature. The most common benign abnormality in the PZ is acute or chronic prostatitis (PI-RADS 2). Prostatitis appears as a nonfocal intermediate signal on the ADC map, often with concurrent diffuse enhancement on DCE-MRI (Fig. 2). Postprostatitis scar tissue has a wedge-shaped or band-like appearance.

Recent prospective, multicenter trials show that mpMRI can obviate unnecessary biopsies by 21–49% in biopsy-naïve men [39–42]. Reported negative mpMRI lesions (PI-RADS 1–2 lesions) should be assessed by the urologist in combination with other clinical parameters and, if deemed necessary, discussed at multidisciplinary team (MDT) meeting. Results from an expert prostate MRI center show

that in only 3%, csPCa was found by a systematic biopsy (SB; predominantly International Society of Urological Pathology [ISUP] grade 2) in men with nonsuspicious mpMRI [41]. Therefore, a "safety net" was provided—a half-yearly PSA test. After 1 yr of follow-up, an additional 1% of csPCa was found, resulting in an mpMRI-negative predictive value (NPV) of 96%. This final 4% figure of false negatives is lower than the recent Cochrane systematic review average (8%), 5% of which are ISUP grade 2 and 3% ISUP grade ≥3, reflecting the expertise of central readings [43].

Regardless, it is clear that template mapping biopsies remains the "gold standard" for the likely pathologic state of the disease. The Cochrane systematic review also analyzed the performance of MRI with template mapping biopsies as a reference standard. The pooled NPV for csPCa (ISUP grade ≥2, prevalence of 30%) was 91% (95% confidence interval: 86–94%) [44]. The PROMIS trial also used transperineal template mapping biopsies and found a lower NPV (76%) [40]. The difference between the pooled and PROMIS data might be attributable to multiple factors including (imaging on 1.5 T MRI and nonadherence to PI-RADS v2 recommendations for imaging), clinical Likert score rather than rule-based imaging PI-RADS assessments, and/or a higher csPCa prevalence [7].

Therefore, when there is a high clinical suspicion of csPCa and negative mpMRI, an SB should be considered and should be discussed with the patient as part of shared decision making [45]. Men with negative mpMRI without a high clinical suspicion (eg, low PSAd) need not undergo immediate biopsy and be safely discharged to their general practitioner (GP), if an adequate safety net of PSA surveillance is implemented, with roles and responsibilities being clearly defined [41,46–48]. Our approach is to advise patients with negative MRI scans who do not undergo immediate biopsy to have 6-monthly PSA tests. If clinical suspicion persists, a re-referral for repeat MRI or an SB should be made.

2.5. Equivocal mpMRI (PI-RADS category 3)

Prevalence rates of PI-RADS 3 assessment in biopsy-naïve men varies between 6% and 39% [41,49]. It is reported that experienced readers have significantly lower rates of PI-RADS 3 scores; thus, the percentage of PI-RADS 3 scorings can be an indicator of reader quality [50]. Radiologic reviews at MDT meetings of equivocal lesions often showed up- or downgrade reclassification [51]. On an individual patient basis, each PI-RADS 3 lesion should be discussed at MDT meetings.

Equivocal lesions pose a diagnostic challenge because even though the proportion of csPCa in this group is low, a considerable percentage of men still have csPCa. The prevalence of csPCa (defined as ISUP grade ≥2) in this category is 4–27% [41,49,52–54]. Similar to PI-RADS 1–2 lesions, clinical risk stratification parameters can aid in decision making on the need to perform a biopsy or rather follow up the lesion with repeated mpMRI and repeated PSA measurements. Elevated PSAd (eg, ≥0.15 ng/ml/ml) has been demonstrated to predict the presence of csPCa for PI-RADS 3 lesions [53–58]. Blood-based and urinary biomarker–incorporated risk models might improve risk stratification, but there is currently insufficient information to advice on the optimal strategy of these men. When decisions are made not to biopsy men with PI-RADS 3 lesions, a "safety net" of imaging and PSA surveillance similar to PI-RADS 1–2 category should be implemented with urologic clinic follow-up (as opposed to GP).

2.6. Suspicious mpMRI (PI-RADS categories 4 and 5)

Using PI-RADS v2, mpMRI can predict the presence of csPCa with high diagnostic accuracy [41,59,60]. On average, in biopsy-naïve men, csPCa (ISUP grade ≥2) is diagnosed in 32–60% for PI-RADS category 4 and 67–83% for PI-RADS category 5 [39,41,42,48,49,54,61,62]. Therefore, PI-RADS 4–5 lesions should always be considered for biopsy if patients are likely to be treated. Whether to perform an SB in addition to an MRDB or only a targeted MRDB in biopsy-naïve men is still debated [47]. The most recent European Association of Urology guideline recommended performing an SB in addition to an MRDB [2]. This approach is supported by a growing body of evidence showing increasing yields with the combined approach in biopsy-naïve men (but not after a prior negative biopsy) [42,63–69]. However, a "focal saturation" approach (ie, multiple cores per suspicious lesion) has been proposed by the PI-RADS Steering Committee as an alternative, which might show similar detection rates of csPCa with the advantages of reducing the detection rates of low-grade PCa and the number of biopsy cores [41,70–74]. In the repeat-biopsy setting, the European and American urological guidelines recommend a target biopsy (in case of PI-RADS scores ≥3), or a case-specific decision, respectively [2,75].

Current literature does not show a significant advantage of one targeted biopsy technique over the others [54,76,77]. However, it should be remembered that these studies were not sufficiently powered to detect differences between techniques for lesions at different locations and by size. Therefore, MR in-bore guided, MR-transrectal ultrasound fusion, or cognitive biopsies can be performed with due consideration of lesion characteristics (size and location), equipment availability, and operators' preference.

Biopsy methods and histopathologic findings should be discussed at MDT meetings attended by radiologists, urologists, and pathologists. Radiologic-pathologic correlations must be performed, and in case of csPCa, appropriate metastatic imaging techniques can be selected according to risk status. Suspicious mpMRI lesions with negative explanatory pathology/low-grade cancer must be re-evaluated, and follow-up with PSA/mpMRI or repeat biopsy should be discussed [12,38]. Insufficient mpMRI quality and reader performance, inaccurate targeting of lesions (sampling error), or undersampling can attribute to undetected csPCa or risk-classification errors [78,79]. False-positive mpMRI (eg, granulomatous prostatitis and reader error) can also occur. In a large retrospective study, follow-up of patients with a negative biopsy after suspicious mpMRI

resulted in the detection of csPCa (defined as ISUP grade ≥2) in 1.7% of men [35].

3. Limitations, challenges, and future developments

Implementation of mpMRI as a triage test before prostate biopsy in biopsy-naïve men has its challenges. Studies showed that mpMRI as triage test is a cost-effective diagnostic approach; however, this is highly dependent on the quality of mpMRI (subsequent MRDB) and health care system [80–82]. PI-RADS (v2) improved standardization of image acquisition and reporting of mpMRI [59,60,83]. However, there remains considerable variation in inter-reader reproducibility, but this is highly dependent on radiologists' experience and training [41,84–88]. Whether the recently published PI-RADS v2.1 improves this needs to be investigated. An appropriate education program, with quality control, is needed for radiologists and urologists. With high-quality standard image acquisition and reading, the proportion of nonsuspicious mpMRI (PI-RADS 1–2) will increase and the number of equivocal lesions will reduce [50,89], although this also is dependent on the csPCa prevalence.

Furthermore, MDT meetings are crucial to discuss radiologic (eg, double read) and histopathologic findings, diagnostic decision making, and choice of an adequate safety net. Prebiopsy multivariate risk stratification using risk calculators, which include PI-RADS, clinical data, pathology, and genomics, needs to be developed and validated. Moreover, guideline recommendations for clinical decision making for each PI-RADS v2.1 category and subsequent biopsy results are needed. Availability and capacity of mpMRI and dedicated radiologists can limit the availability of mpMRI in daily clinical practice [45]. To shorten examination time, biparametric MRI (ie, omitting DCE-MRI) to exclude csPCa in biopsy-naïve men is increasingly being investigated, with promising initial results [90–92]. Biparametric MRI could reduce scan times and save cost for contrast agent injection, but data of prospective multireader trials in nonexpert centers are missing to routinely recommend this approach.

4. Conclusions

In addition to the previous "surgery-in-motion" video that shows how optimal mpMR images are acquired, this video also shows how the radiologists perform their interpretations. To enhance standardization, lesions must be scored using the PI-RADS assessment system. TZ lesions that show "erased charcoal" or disruption of "organized chaos," and PZ lesions that are "black" on the ADC map and "white" on the high *b*-value DWI should be evaluated for a likelihood of csPCa using the PI-RADS system. When mpMRI is of good quality and is evaluated according to the PI-RADS v2.1 recommendations, this technique adds valuable information to other clinical data and can be used to reliably exclude csPCa, and so to avoid a biopsy and indicate where MRDB cores should be targeted. The next video discusses these biopsy options (MR-targeted biopsy video).

***Author contributions*:** Jelle O. Barentsz had full access to all the data in the study and takes responsibility for the integrity of the data and the accuracy of the data analysis.

Study concept and design: Israël, van der Leest, Sedelaar, Padhani, Zámecnik, Barentsz.
Acquisition of data: Israël, van der Leest, Barentsz.
Analysis and interpretation of data: Israël, van der Leest, Sedelaar, Padhani, Zámecnik, Barentsz.
Drafting of the manuscript: Israël, van der Leest, Barentsz.
Critical revision of the manuscript for important intellectual content: Israël, van der Leest, Sedelaar, Padhani, Zámecnik, Barentsz.
Statistical analysis: Israël, van der Leest, Sedelaar, Padhani, Zámecnik, Barentsz.
Obtaining funding: None.
Administrative, technical, or material support: Barentsz.
Supervision: Barentsz.
Other: None.

Financial disclosures: Jelle O. Barentsz certifies that all conflicts of interest, including specific financial interests and relationships and affiliations relevant to the subject matter or materials discussed in the manuscript (eg, employment/affiliation, grants or funding, consultancies, honoraria, stock ownership or options, expert testimony, royalties, or patents filed, received, or pending), are the following: None.

***Funding/Support and role of the sponsor*:** This work was supported by Soteria Medical.

***Acknowledgments*:** We like to thank Soteria Medical (Arnhem, the Netherlands) for their assistance in producing the video.

Appendix A. Supplementary data

Supplementary material related to this article can be found, in the online version, at doi:https://doi.org/10.1016/j.eururo.2019.10.024.

References

[1] Hricak H, Choyke PL, Eberhardt SC, Leibel SA, Scardino PT. Imaging prostate cancer: a multidisciplinary perspective. Radiology 2007;243:28–53.
[2] Mottet N, van den Bergh RCN, Briers E, et al. EAU – ESTRO – ESUR – SIOG guidelines on prostate cancer 2019. In: European Association of Urology guidelines, editor. Presented at the EAU Annual Congress Barcelona 2019. Arnhem, The Netherlands: European Association of Urology Guidelines Office; 2019.
[3] Briganti A, Fossati N, Catto JWF, et al. Active surveillance for low-risk prostate cancer: the European Association of Urology position in 2018. Eur Urol 2018;74:357–68.
[4] Kitajima K, Hartman RP, Froemming AT, Hagen CE, Takahashi N, Kawashima A. Detection of local recurrence of prostate cancer after radical prostatectomy using endorectal coil MRI at 3 T: addition of DWI and dynamic contrast enhancement to T2-weighted MRI. AJR Am J Roentgenol 2015;205:807–16.

[5] Schmidt MA, Payne GS. Radiotherapy planning using MRI. Phys Med Biol 2015;60:R323–61.
[6] Ko YH, Song PH, Moon KH, Jung HC, Cheon J, Sung DJ. The optimal timing of post-prostate biopsy magnetic resonance imaging to guide nerve-sparing surgery. Asian J Androl 2014;16:280–4.
[7] Weinreb JC, Barentsz JO, Choyke PL, et al. PI-RADS Prostate Imaging - Reporting and Data System: 2015, version 2. Eur Urol 2016;69:16–40.
[8] Walz J, Epstein JI, Ganzer R, et al. A critical analysis of the current knowledge of surgical anatomy of the prostate related to optimisation of cancer control and preservation of continence and erection in candidates for radical prostatectomy: an update. Eur Urol 2016;70:301–11.
[9] Chen ME, Johnston DA, Tang K, Babaian RJ, Troncoso P. Detailed mapping of prostate carcinoma foci: biopsy strategy implications. Cancer 2000;89:1800–9.
[10] McNeal JE, Redwine EA, Freiha FS, Stamey TA. Zonal distribution of prostatic adenocarcinoma. Correlation with histologic pattern and direction of spread. Am J Surg Pathol 1988;12:897–906.
[11] Akin O, Sala E, Moskowitz CS, et al. Transition zone prostate cancers: features, detection, localization, and staging at endorectal MR imaging. Radiology 2006;239:784–92.
[12] Rosenkrantz AB, Taneja SS. Radiologist, be aware: ten pitfalls that confound the interpretation of multiparametric prostate MRI. AJR Am J Roentgenol 2014;202:109–20.
[13] Panebianco V, Giganti F, Kitzing YX, et al. An update of pitfalls in prostate mpMRI: a practical approach through the lens of PI-RADS v. 2 guidelines. Insights Imaging 2018;9:87–101.
[14] Barentsz JO, Richenberg J, Clements R, et al. ESUR prostate MR guidelines 2012. Eur Radiol 2012;22:746–57.
[15] Barentsz JO, Weinreb JC, Verma S, et al. Synopsis of the PI-RADS v2 guidelines for multiparametric prostate magnetic resonance imaging and recommendations for use. Eur Urol 2016;69:41–9.
[16] Ren J, Huan Y, Wang H, et al. Diffusion-weighted imaging in normal prostate and differential diagnosis of prostate diseases. Abdom Imaging 2008;33:724–8.
[17] Hambrock T, Somford DM, Huisman HJ, et al. Relationship between apparent diffusion coefficients at 3.0-T MR imaging and Gleason grade in peripheral zone prostate cancer. Radiology 2011;259:453–61.
[18] Downes MR, Gibson E, Sykes J, Haider M, van der Kwast TH, Ward A. Determination of the association between T2-weighted MRI and Gleason sub-pattern: a proof of principle study. Acad Radiol 2016;23:1412–21.
[19] De Visschere PJ, Vral A, Perletti G, et al. Multiparametric magnetic resonance imaging characteristics of normal, benign and malignant conditions in the prostate. Eur Radiol 2017;27:2095–109.
[20] Qayyum A. Diffusion-weighted imaging in the abdomen and pelvis: concepts and applications. Radiographics 2009;29:1797–810.
[21] Langer DL, van der Kwast TH, Evans AJ, et al. Prostate tissue composition and MR measurements: investigating the relationships between ADC, T2, K(trans), v(e), and corresponding histologic features. Radiology 2010;255:485–94.
[22] Feuerlein S, Davenport MS, Krishnaraj A, Merkle EM, Gupta RT. Computed high b-value diffusion-weighted imaging improves lesion contrast and conspicuity in prostate cancer. Prostate Cancer Prostatic Dis 2015;18:155–60.
[23] Wetter A, Nensa F, Lipponer C, et al. High and ultra-high b-value diffusion-weighted imaging in prostate cancer: a quantitative analysis. Acta Radiol 2015;56:1009–15.
[24] Kim JH, Kim JK, Park BW, Kim N, Cho KS. Apparent diffusion coefficient: prostate cancer versus noncancerous tissue according to anatomical region. J Magn Reson Imaging 2008;28:1173–9.
[25] Tamada T, Sone T, Toshimitsu S, et al. Age-related and zonal anatomical changes of apparent diffusion coefficient values in normal human prostatic tissues. J Magn Reson Imaging 2008;27:552–6.
[26] Turkbey B, Shah VP, Pang Y, et al. Is apparent diffusion coefficient associated with clinical risk scores for prostate cancers that are visible on 3-T MR images? Radiology 2011;258:488–95.
[27] Boesen L, Chabanova E, Logager V, Balslev I, Thomsen HS. Apparent diffusion coefficient ratio correlates significantly with prostate cancer Gleason score at final pathology. J Magn Reson Imaging 2015;42:446–53.
[28] Hambrock T, Hoeks C, Hulsbergen-van de Kaa C, et al. Prospective assessment of prostate cancer aggressiveness using 3-T diffusion-weighted magnetic resonance imaging-guided biopsies versus a systematic 10-core transrectal ultrasound prostate biopsy cohort. Eur Urol 2012;61:177–84.
[29] Oto A, Kayhan A, Jiang Y, et al. Prostate cancer: differentiation of central gland cancer from benign prostatic hyperplasia by using diffusion-weighted and dynamic contrast-enhanced MR imaging. Radiology 2010;257:715–23.
[30] Verma S, Turkbey B, Muradyan N, et al. Overview of dynamic contrast-enhanced MRI in prostate cancer diagnosis and management. AJR Am J Roentgenol 2012;198:1277–88.
[31] Huisman HJ, Engelbrecht MR, Barentsz JO. Accurate estimation of pharmacokinetic contrast-enhanced dynamic MRI parameters of the prostate. J Magn Reson Imaging 2001;13:607–14.
[32] Oppenheimer DC, Weinberg EP, Hollenberg GM, Meyers SP. Multiparametric magnetic resonance imaging of recurrent prostate cancer. J Clin Imaging Sci 2016;6:18.
[33] Barrett T, Vargas HA, Akin O, Goldman DA, Hricak H. Value of the hemorrhage exclusion sign on T1-weighted prostate MR images for the detection of prostate cancer. Radiology 2012;263:751–7.
[34] Turkbey B, Rosenkrantz AB, Haider MA, et al. Prostate Imaging Reporting and Data System Version 2.1: 2019 update of Prostate Imaging Reporting and Data System Version 2. Eur Urol 2019;76:340–51.
[35] Venderink W, van Luijtelaar A, Bomers JG, et al. Results of targeted biopsy in men with magnetic resonance imaging lesions classified equivocal, likely or highly likely to be clinically significant prostate cancer. Eur Urol 2017;73:353–60.
[36] Li Y, Mongan J, Behr SC, et al. Beyond prostate adenocarcinoma: expanding the differential diagnosis in prostate pathologic conditions. Radiographics 2016;36:1055–75.
[37] Panebianco V, Barchetti F, Barentsz J, et al. Pitfalls in interpreting mp-MRI of the prostate: a pictorial review with pathologic correlation. Insights Imaging 2015;6:611–30.
[38] Kitzing YX, Prando A, Varol C, Karczmar GS, Maclean F, Oto A. Benign conditions that mimic prostate carcinoma: MR imaging features with histopathologic correlation. Radiographics 2016;36:162–75.
[39] Kasivisvanathan V, Rannikko AS, Borghi M, et al. MRI-targeted or standard biopsy for prostate-cancer diagnosis. N Engl J Med 2018;378:1767–77.
[40] Ahmed HU, El-Shater Bosaily A, Brown LC, et al. Diagnostic accuracy of multi-parametric MRI and TRUS biopsy in prostate cancer (PROMIS): a paired validating confirmatory study. Lancet 2017;389:815–22.
[41] van der Leest M, Cornel E, Israel B, et al. Head-to-head comparison of transrectal ultrasound-guided prostate biopsy versus multiparametric prostate resonance imaging with subsequent magnetic resonance-guided biopsy in biopsy-naive men with elevated prostate-specific antigen: a large prospective multicenter clinical study. Eur Urol 2019;75:570–8.
[42] Rouviere O, Puech P, Renard-Penna R, et al. Use of prostate systematic and targeted biopsy on the basis of multiparametric MRI in

biopsy-naive patients (MRI-FIRST): a prospective, multicentre, paired diagnostic study. Lancet Oncol 2019;20:100–9.
[43] Drost FH, Osses DF, Nieboer D, et al. Prostate MRI, with or without MRI-targeted biopsy, and systematic biopsy for detecting prostate cancer. Cochrane Database Syst Rev 2019;4:CD012663.
[44] Drost FH, Osses D, Nieboer D , et al. Prostate magnetic resonance imaging, with or without magnetic resonance imaging-targeted biopsy, and systematic biopsy for detecting prostate cancer: a Cochrane systematic review and meta-analysis. Eur Urol 2020;77:78–94.
[45] Padhani AR, Weinreb J, Rosenkrantz AB, Villeirs G, Turkbey B, Barentsz J. Prostate Imaging-Reporting and Data System Steering Committee: PI-RADS v2 status update and future directions. Eur Urol 2019;75:385–96.
[46] Oishi M, Shin T, Ohe C, et al. Which patients with negative magnetic resonance imaging can safely avoid biopsy for prostate cancer? J Urol 2019;201:268–77.
[47] Brizmohun Appayya M, Adshead J, Ahmed HU, et al. National implementation of multi-parametric magnetic resonance imaging for prostate cancer detection—recommendations from a UK consensus meeting. BJU Int 2018;122:13–25.
[48] Panebianco V, Barchetti G, Simone G, et al. Negative multiparametric magnetic resonance imaging for prostate cancer: what's next? Eur Urol 2018;74:48–54.
[49] Schoots IG. MRI in early prostate cancer detection: how to manage indeterminate or equivocal PI-RADS 3 lesions? Transl Androl Urol 2018;7:70–82.
[50] Greer MD, Brown AM, Shih JH, et al. Accuracy and agreement of PIRADSv2 for prostate cancer mpMRI: A multireader study. J Magn Reson Imaging 2017;45:579–85.
[51] Steinkohl F, Gruber L, Bektic J, et al. Retrospective analysis of the development of PIRADS 3 lesions over time: when is a follow-up MRI reasonable? World J Urol 2018;36:367–73.
[52] Sheridan AD, Nath SK, Syed JS, et al. Risk of clinically significant prostate cancer associated with Prostate Imaging Reporting and Data System category 3 (equivocal) lesions identified on multiparametric prostate MRI. AJR Am J Roentgenol 2018;210:347–357.
[53] Ullrich T, Quentin M, Arsov C, et al. Risk stratification of equivocal lesions on multiparametric magnetic resonance imaging of the prostate. J Urol 2018;199:691–8.
[54] Venderink W, van der Leest M, van Luijtelaar A, et al. Retrospective comparison of direct in-bore magnetic resonance imaging (MRI)-guided biopsy and fusion-guided biopsy in patients with MRI lesions which are likely or highly likely to be clinically significant prostate cancer. World J Urol 2017;35:1849–55.
[55] Brizmohun Appayya M, Sidhu HS, Dikaios N, et al. Characterizing indeterminate (Likert-score 3/5) peripheral zone prostate lesions with PSA density, PI-RADS scoring and qualitative descriptors on multiparametric MRI. Br J Radiol 2018;91:20170645.
[56] Washino S, Okochi T, Saito K, et al. Combination of Prostate Imaging Reporting and Data System (PI-RADS) score and prostate-specific antigen (PSA) density predicts biopsy outcome in prostate biopsy naive patients. BJU Int 2017;119:225–33.
[57] Rais-Bahrami S, Siddiqui MM, Vourganti S, et al. Diagnostic value of biparametric magnetic resonance imaging (MRI) as an adjunct to prostate-specific antigen (PSA)-based detection of prostate cancer in men without prior biopsies. BJU Int 2015;115:381–8.
[58] Felker ER, Raman SS, Margolis DJ, et al. Risk stratification among men with Prostate Imaging Reporting and Data System version 2 category 3 transition zone lesions: is biopsy always necessary? AJR Am J Roentgenol 2017;209:1272–7.
[59] Zhang L, Tang M, Chen S, Lei X, Zhang X, Huan Y. A meta-analysis of use of Prostate Imaging Reporting and Data System version 2 (PI-RADS V2) with multiparametric MR imaging for the detection of prostate cancer. Eur Radiol 2017;27:5204–14.
[60] Woo S, Suh CH, Kim SY, Cho JY, Kim SH. Diagnostic Performance of Prostate Imaging Reporting and Data System Version 2 for detection of prostate cancer: a systematic review and diagnostic meta-analysis. Eur Urol 2017;72:177–88.
[61] Mehralivand S, Bednarova S, Shih JH, et al. Prospective evaluation of PI-RADS version 2 using the International Society of Urological Pathology Prostate Cancer Grade Group system. J Urol 2017;198:583–90.
[62] Moldovan PC, Van den Broeck T, Sylvester R, et al. What is the negative predictive value of multiparametric magnetic resonance imaging in excluding prostate cancer at biopsy? A systematic review and meta-analysis from the European Association of Urology Prostate Cancer Guidelines Panel. Eur Urol 2017;72:250–66.
[63] Maxeiner A, Kittner B, Blobel C, et al. Primary magnetic resonance imaging/ultrasonography fusion-guided biopsy of the prostate. BJU Int 2018;122:211–8.
[64] Ploussard G, Borgmann H, Briganti A, et al. Positive pre-biopsy MRI: are systematic biopsies still useful in addition to targeted biopsies? World J Urol 2019;37(2):243–51.
[65] Washino S, Kobayashi S, Okochi T, et al. Cancer detection rate of prebiopsy MRI with subsequent systematic and targeted biopsy are superior to non-targeting systematic biopsy without MRI in biopsy naive patients: a retrospective cohort study. BMC Urol 2018;18:51.
[66] Hansen NL, Barrett T, Kesch C, et al. Multicentre evaluation of magnetic resonance imaging supported transperineal prostate biopsy in biopsy-naive men with suspicion of prostate cancer. BJU Int 2018;122:40–9.
[67] Radtke JP, Schwab C, Wolf MB, et al. Multiparametric magnetic resonance imaging (MRI) and MRI-transrectal ultrasound fusion biopsy for index tumor detection: correlation with radical prostatectomy specimen. Eur Urol 2016;70:846–53.
[68] Hofbauer SL, Maxeiner A, Kittner B, et al. Validation of Prostate Imaging Reporting and Data System version 2 for the detection of prostate cancer. J Urol 2018;200:767–73.
[69] Stabile A, Giganti F, Emberton M, Moore CM. MRI in prostate cancer diagnosis: do we need to add standard sampling? A review of the last 5 years. Prostate Cancer Prostatic Dis 2018;21:473–87.
[70] Calio BP, Sidana A, Sugano D, et al. Risk of upgrading from prostate biopsy to radical prostatectomy pathology—does saturation biopsy of index lesion during multiparametric magnetic resonance imaging-transrectal ultrasound fusion biopsy help? J Urol 2018;199:976–82.
[71] Muthigi A, George AK, Sidana A, et al. Missing the mark: prostate cancer upgrading by systematic biopsy over magnetic resonance imaging/transrectal ultrasound fusion biopsy. J Urol 2017;197:327–34.
[72] Lu AJ, Syed JS, Ghabili K, et al. Role of core number and location in targeted magnetic resonance imaging-ultrasound fusion prostate biopsy. Eur Urol 2019;76:14–7.
[73] Zhang M, Milot L, Khalvati F, et al. Value of increasing biopsy cores per target with cognitive MRI-targeted transrectal US prostate biopsy. Radiology 2019;291:83–9.
[74] Padhani AR, Barentsz J, Villeirs G, et al. PI-RADS Steering Committee: the PI-RADS multiparametric MRI and MRI-directed biopsy pathway. Radiology 2019;292:464–74.
[75] Rosenkrantz AB, Verma S, Choyke P, et al. Prostate magnetic resonance imaging and magnetic resonance imaging targeted biopsy in patients with a prior negative biopsy: a consensus statement by AUA and SAR. J Urol 2016;196:1613–8.
[76] Wegelin O, van Melick HHE, Hooft L, et al. Comparing three different techniques for magnetic resonance imaging-targeted prostate biopsies: a systematic review of in-bore versus magnetic resonance

imaging-transrectal ultrasound fusion versus cognitive registration. Is there a preferred technique? Eur Urol 2017;71:517–31.
[77] Wegelin O, Exterkate L, van der Leest M, et al. The FUTURE trial: a multicenter randomised controlled trial on target biopsy techniques based on magnetic resonance imaging in the diagnosis of prostate cancer in patients with prior negative biopsies. Eur Urol 2019;75:582–90.
[78] Kenigsberg AP, Renson A, Rosenkrantz AB, et al. Optimizing the number of cores targeted during prostate magnetic resonance imaging fusion target biopsy. Eur Urol Oncol 2018;1:418–25.
[79] Porpiglia F, De Luca S, Passera R, et al. Multiparametric magnetic resonance/ultrasound fusion prostate biopsy: number and spatial distribution of cores for better index tumor detection and characterization. J Urol 2017;198:58–64.
[80] Pahwa S, Schiltz NK, Ponsky LE, Lu Z, Griswold MA, Gulani V. Cost-effectiveness of MR imaging-guided strategies for detection of prostate cancer in biopsy-naive men. Radiology 2017;285:157–66.
[81] Faria R, Soares MO, Spackman E, et al. optimising the diagnosis of prostate cancer in the era of multiparametric magnetic resonance imaging: a cost-effectiveness analysis based on the Prostate MR Imaging Study (PROMIS). Eur Urol 2018;73:23–30.
[82] de Rooij M, Crienen S, Witjes JA, Barentsz JO, Rovers MM, Grutters JP. Cost-effectiveness of magnetic resonance (MR) imaging and MR-guided targeted biopsy versus systematic transrectal ultrasound-guided biopsy in diagnosing prostate cancer: a modelling study from a health care perspective. Eur Urol 2014;66:430–6.
[83] Chen F, Cen S, Palmer S. Application of Prostate Imaging Reporting and Data System version 2 (PI-RADS v2): interobserver agreement and positive predictive value for localization of intermediate- and high-grade prostate cancers on multiparametric magnetic resonance imaging. Acad Radiol 2017;24:1101–6.
[84] Glazer DI, Mayo-Smith WW, Sainani NI, et al. Interreader agreement of Prostate Imaging Reporting and Data System version 2 using an in-bore MRI-guided prostate biopsy cohort: a single institution's initial experience. AJR Am J Roentgenol 2017;209:W145–51.
[85] Rosenkrantz AB, Ginocchio LA, Cornfeld D, et al. Interobserver reproducibility of the PI-RADS version 2 lexicon: a multicenter study of six experienced prostate radiologists. Radiology 2016;280:793–804.
[86] Shankar PR, Kaza RK, Al-Hawary MM, et al. Impact of clinical history on maximum PI-RADS version 2 score: a six-reader 120-case sham history retrospective evaluation. Radiology 2018;288:158–63.
[87] Purysko AS, Bittencourt LK, Bullen JA, Mostardeiro TR, Herts BR, Klein EA. Accuracy and interobserver agreement for Prostate Imaging Reporting and Data System, version 2, for the characterization of lesions identified on multiparametric MRI of the prostate. AJR Am J Roentgenol 2017;209:339–49.
[88] Mussi TC, Yamauchi FI, Tridente CF, et al. Interobserver agreement and positivity of PI-RADS version 2 among radiologists with different levels of experience. Acad Radiol 2019;26:1017–22.
[89] Garcia-Reyes K, Passoni NM, Palmeri ML, et al. Detection of prostate cancer with multiparametric MRI (mpMRI): effect of dedicated reader education on accuracy and confidence of index and anterior cancer diagnosis. Abdom Imaging 2015;40:134–42.
[90] Woo S, Suh CH, Kim SY, Cho JY, Kim SH, Moon MH. Head-to-Head comparison between biparametric and multiparametric MRI for the diagnosis of prostate cancer: a systematic review and meta-analysis. AJR Am J Roentgenol 2018;211:W226–41.
[91] Boesen L, Norgaard N, Logager V, et al. Assessment of the diagnostic accuracy of biparametric magnetic resonance imaging for prostate cancer in biopsy-naive men: the Biparametric MRI for Detection of Prostate Cancer (BIDOC) study. JAMA Netw Open 2018;1:e180219.
[92] van der Leest M, Israel B, Cornel EB, et al. High diagnostic performance of short magnetic resonance imaging protocols for prostate cancer detection in biopsy-naive men: the next step in magnetic resonance imaging accessibility. Eur Urol 2019;76:574–81.